



## Design of an innovative vacuum evaporator system for brine concentration assisted by software tool simulation

D. Xevgenos\*, P. Michailidis, K. Dimopoulos, M. Krokida, M. Loizidou

*Unit of Environmental Science & Technology, School of Chemical Engineering, National Technical University of Athens, Zographou Campus, 9, Heroon Polytechniou Str., 15773 Athens, Greece, Tel. +30 210 772 3108; Fax: +30 210 772 3285; emails: xevgenos@central.ntua.gr (D. Xevgenos); kostas.dimopoulos@gmail.com (K. Dimopoulos)*

Received 19 October 2013; Accepted 15 July 2014

---

### ABSTRACT

In this paper, the design of a novel multi-effect distillation system is described for the concentration of the brine effluent produced from desalination plants. The evaporation process was simulated through the use of a software tool that was developed for the brine treatment process. The results and the simulator tool are also discussed in the paper. The evaporator unit comprises the first treatment stage of a pilot system that was developed in the framework of the SOL-BRINE project. The system is based on the zero liquid discharge principle and is operated through the use of renewable sources and, in particular, solar energy. The system has been installed in Tinos Island, Greece and is operating regularly since January 2013.

*Keywords:* Evaporator; Brine effluent; Zero liquid discharge; Simulator tool; Design

---

### 1. Introduction

The desalination process involves a large volume of wastewater: around 2L of brine for every liter of freshwater produced. This wastewater poses a significant discharge problem in terms of both volume and high salt concentration. The adverse effects of brine have been studied by many researchers and are increasingly considered when selecting the desalination plant site [1]. The problem is even bigger with an inland desalination plant, where the brine effluent is usually rejected through deep well injection, affecting adversely the state of underground aquifers [2].

With respect to brine management, various practices have been applied such as land application,

evaporative ponds, surface water disposal, or deep well injection [1]. Zero liquid discharge is an approach which aims to eliminate the brine effluent and thus brine disposal needs. In order to do so, it is obligatory to reach high concentration levels, up to total dissolved solids (TDS) levels of 260,000 ppm. The only option to achieve this is through evaporation, given that membranes present high fouling risk at high concentration levels. As a result, at cases where volume minimization or elimination of brine is concerned, evaporation of the effluent is considered [3]. For instance, evaporation ponds comprise one of the most popular brine disposal techniques [2]. However, this implies land availability and suitable climate conditions (dry climate, sufficient insolation). In cases, where there are land availability limitations such as

---

\*Corresponding author.

*Presented at the International Conference WIN4Life, 19–21 September 2013, Tinos Island, Greece*

1944-3994/1944-3986 © 2014 The Author(s). Published by Balaban Desalination Publications.

This is an Open Access article. Non-commercial re-use, distribution, and reproduction in any medium, provided the original work is properly attributed, cited, and is not altered, transformed, or built upon in any way, is permitted. The moral rights of the named author(s) have been asserted.

islands or where the cost of land is prohibitive, evaporation ponds cannot offer an integrated brine management solution.

## 2. Design of the evaporator unit

Within the SOL-BRINE project (LIFE09 ENV/GR/000299), a zero liquid discharge system has been developed comprising: (a) an evaporator unit; (b) a crystallizer unit; and (c) a dryer. In this paper, the innovative design of the evaporator unit is discussed, including an integrated process simulator software as developed during the SOL-BRINE project.

### 2.1. General design considerations

The brine from the reverse osmosis unit at Agios Fokas area in Tinos Island, Greece is fed in the vacuum evaporation system. The evaporator comprises the first treatment stage of the innovative brine treatment process. The feed showed a TDS of nominally 60,000 ppm.

The purpose of the evaporation system is to increase the salt content of the feed from 6% close to the saturation point (~26%). This is achieved by vaporization of water (solvent) while the solute (salts) remains in the concentrated solution, which is further treated at the second stage, the crystallizer unit. It must be noted that the vast majority of the water quantity (almost 80% of the water) is evaporated and recovered during the first treatment stage.

Concentrated brine could also be obtained by treating the RO brine in an evaporation pond. Although this process presents practically no running costs, it requires large land availability and considerable evaporation time. Assuming a relatively high evaporation rate of 0.11/h/m<sup>2</sup> or approximately 11/d, a land surface of approximately 500 m<sup>2</sup> is required for evaporating 500 L of brine. The developed evaporation system has minimum land requirements and accelerates the whole evaporation process. The evaporator requires less than 5 m<sup>2</sup>, which corresponds to two orders of magnitude, which is less compared with evaporation ponds. Furthermore, the process is not affected by weather conditions, such as rain or variable insolation (e.g. cloudy weather).

The evaporation system comprises two consecutive effects. The purpose of using two effects is to economize on energy consumption. Each evaporator consists of a heat exchanger and a vessel for the separation of liquid–vapor phase. The cold feed stream takes up heat through condensation of water vapor. The absorbed heat causes vaporization of water and an

increase of the concentration level of the brine stream. The vapor is then condensed and recovered as distillate water. The evaporator unit has a forward-feed arrangement, meaning that both the concentrated solution and the vapor streams go from the first effect to the last. The concentrated brine is withdrawn from the last effect and pumped to the crystallizer unit.

Furthermore, boiling point elevation has been considered. A preheater is used for heating the feed stream of the first effect up to a temperature close to its boiling point. The first effect is heated by an external heat source; in our case, from hot water produced by a solar field of evacuated tube collectors. Energy recovered from the vaporized solvent is used for heating the second effect. A schematic diagram of the evaporator unit is shown in Fig. 1.

### 2.2. Process simulator

In order to design the main system components, a special simulator software tool was developed [4]. The system process model was based on a set of 10 design variables (five design variables for the evaporator design).

The software tool can predict the values of key operating parameters according to the specified inputs of the design variables. The tool integrates mass and energy balances, process equipment parameters, cost estimation, and environmental aspects of the units involved. The simulator with the process flow diagram showing the sequence of equipment and unit operations is presented in Fig. 2. It must be noticed that the simulator tool has been developed in Microsoft Excel environment (Visual Basic) and can be downloaded from the project website (<http://uest.ntua.gr/solbrine/>). The process simulator allows to select between (a) two or three effects in the evaporator, (b) the use of mechanical vapor compression or thermal vapor compression in the evaporator and crystallizer units, etc. The reader can find more information on how to use the software tool in the respective deliverable of the SOL-BRINE project (Deliverable 2.4).

With reference to the evaporator unit, the tool enables to determine the concentration of the input stream and solves all mass and energy balance equations as to achieve 26% concentration in the exit stream. This is obtained through an integrated iteration process and results from the design philosophy of the pilot system (see Fig. 3). This is based on the fact that the exit stream from the evaporator is targeted to be near saturation. The almost saturated solution enters the crystallizer and through a restricted additional evaporation, the first solid salt crystals will be

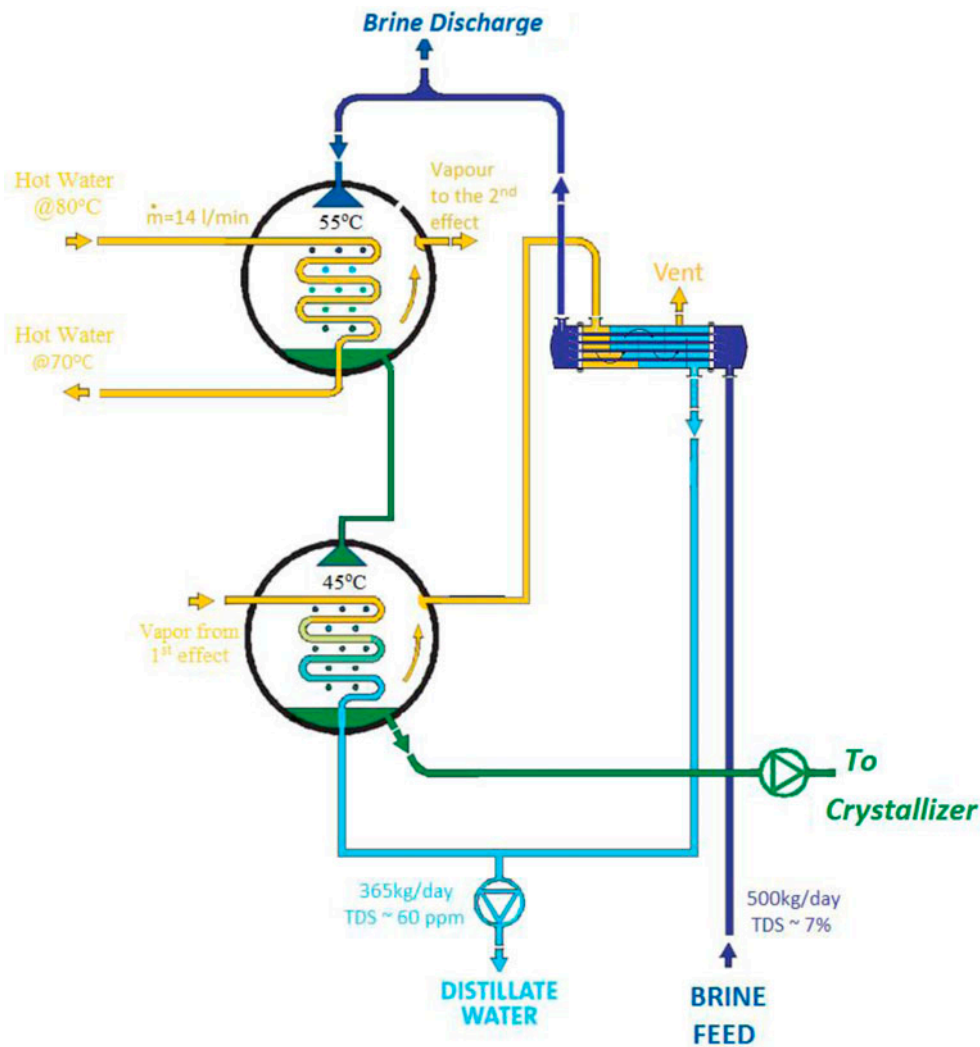


Fig. 1. Schematic diagram of the innovative vacuum evaporator unit, SOL-BRINE project.

precipitated within the crystallizer unit and not within the evaporator.

### 2.3. Mathematical modeling

A mathematical model was developed for a triple-effect evaporator, incorporating geometrical, operating, and self-balancing variables [4]. The equations involve: (a) material balance; (b) boiling point elevation; and (c) energy balance.

#### 2.3.1. Material balance

$$L_0 X_0 = L_1 X_1 \tag{1}$$

$$L_1 X_1 = L_2 X_2 \tag{2}$$

$$L_2 X_2 = L_3 X_3 \tag{3}$$

where  $L_0$  is the inlet flow rate of the solution,  $L_1$ ,  $L_2$ , and  $L_3$  are the flow rate of the solution at the exit of each effect,  $X_0$  is the initial concentration of the solution, and  $X_1$ ,  $X_2$ , and  $X_3$  are the concentration of the solution at the exit of each effect.

These equations express the material balance of the dissolved salt in the 1st, 2nd, and 3rd effect of the evaporator, respectively. The mass flow of solid material (salts) entering and leaving the evaporator is equal in the steady state.

They calculate the mass flow rate of the solvent between the effects as well as in the exit of the evaporator.

$$L_0 = L_1 + V_1 \tag{4}$$

$$L_1 = L_2 + V_2 \tag{5}$$

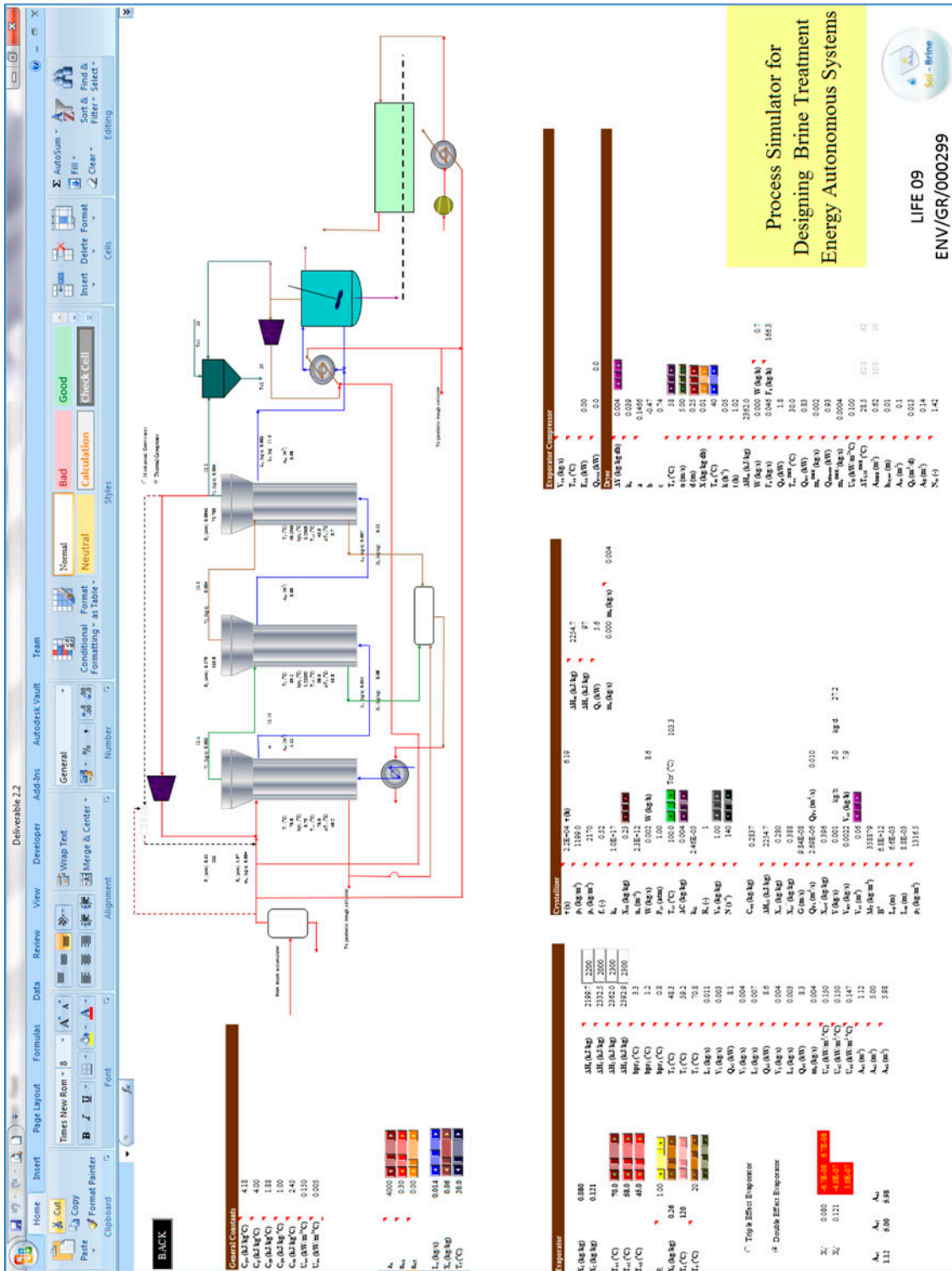


Fig. 2. Process simulator developed within the SOL-BRINE project. Notes: The process simulator tool is available at: [uest.ntua.gr/solbrine/uploads/files/Deliverable2.2.xls](http://uest.ntua.gr/solbrine/uploads/files/Deliverable2.2.xls).

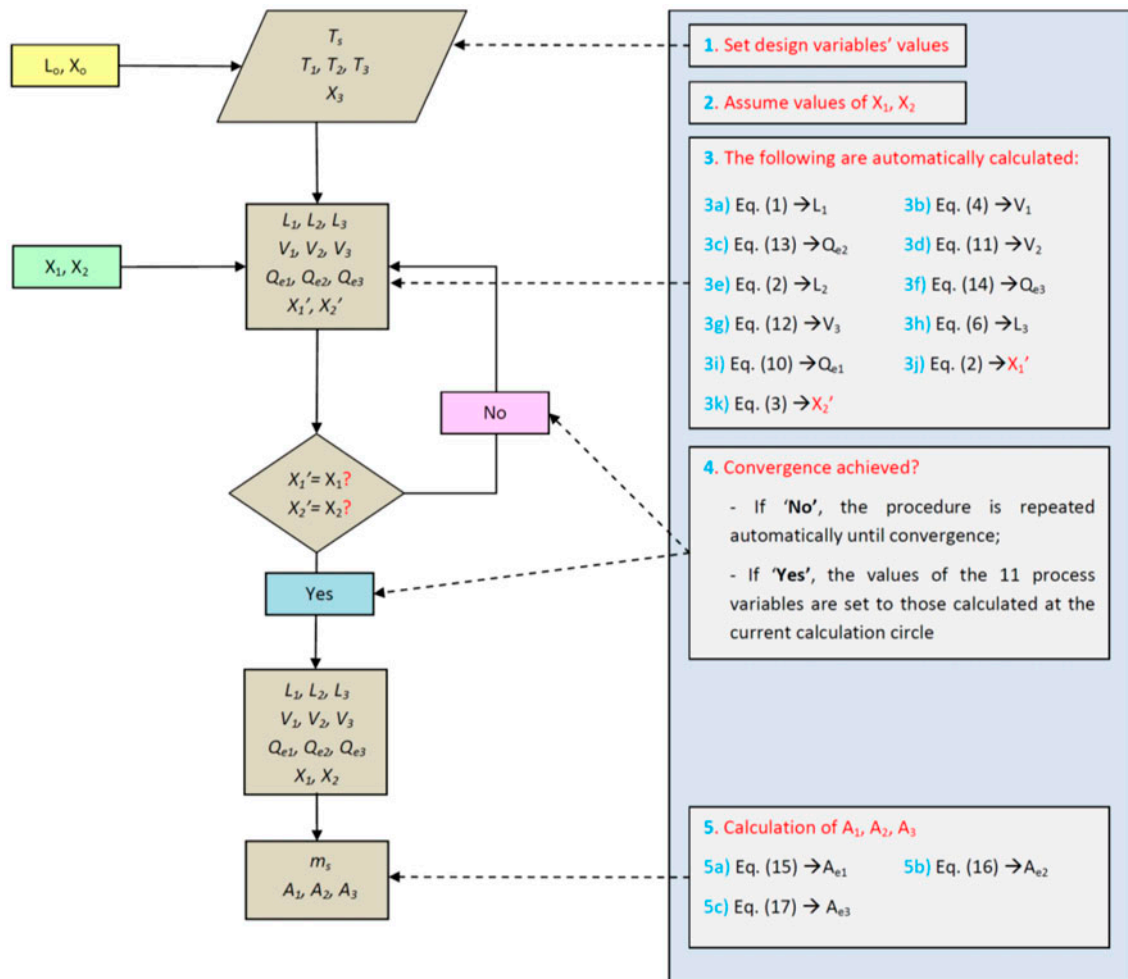


Fig. 3. Calculations flow used in the simulation tool.  
 Notes: For the equations presented in the box on the right, see section 0.

$$L_2 = L_3 + V_3 \tag{6}$$

The above three equations represent the total material balance in each effect and calculate each effect's vapor flow.

$V_1$ ,  $V_2$ , and  $V_3$  are the vapor flow rates in the 1st, 2nd, and 3rd effect, respectively.

2.3.2. Boiling point elevation

$$T_1 = T_{w1} + bpr_1 \tag{7}$$

$$T_2 = T_{w2} + bpr_2 \tag{8}$$

$$T_3 = T_{w3} + bpr_3 \tag{9}$$

These equations present the temperature of the solution in each effect. This temperature is affected by the pressure of the effect thought  $T_{wi}$ , which is the boiling point at the corresponding pressure, and the boiling point elevation caused by the salts present in the solution.

- $T_1$ ,  $T_2$ , and  $T_3$  are the actual temperatures in each effect of the evaporator,
- $T_{w1}$ ,  $T_{w2}$ , and  $T_{w3}$  are the temperatures of each effect corresponding to its pressure, and
- $bpr_1$ ,  $bpr_2$ , and  $bpr_3$  are the boiling point elevations of the solution in its effect.

### 2.3.3. Energy balance

$$Q_{e1} = L_0 C_p (T_1 - T_0) + V_1 \Delta H_{T_{w1}} \quad (10)$$

$$Q_{e2} = L_1 C_p (T_2 - T_1) + V_2 \Delta H_{T_{w2}} \quad (11)$$

$$Q_{e3} = L_2 C_p (T_3 - T_2) + V_3 \Delta H_{T_{w3}} \quad (12)$$

The above equations express the energy balances in each effect of the evaporator, where  $Q_{e1}$ ,  $Q_{e2}$ , and  $Q_{e3}$  are the heat fluxes in each effect,  $\Delta H_{T_{w1}}$ ,  $\Delta H_{T_{w2}}$ , and  $\Delta H_{T_{w3}}$  are the heat of vaporization of the solvent in the corresponding pressure of each effect, and,  $C_p$  is the heat capacity of the solution.

The energy (heat) presented in each effect is the sum of the heat offered by the steam of the previous effect or the flash/compressor in the case of the first effect and the heat produced by the introduction of the solution in an effect of lower pressure. Especially in the case of the first effect, an additional amount of heat has to be offered in most of the cases for the heating of the solution till the temperature in the first effect.

$$Q_{e2} = V_1 \Delta H_{T_{w1}} \quad (13)$$

$$Q_{e3} = V_2 \Delta H_{T_{w2}} \quad (14)$$

These two equations present the heat flux in the second and third effect produced by the vapor condensation coming from the previous effect.

$$Q_{e1} = A_{e1} U_{e1} (T_s - T_1) \quad (15)$$

$$Q_{e2} = A_{e2} U_{e2} (T_{w1} - T_2) \quad (16)$$

$$Q_{e3} = A_{e3} U_{e3} (T_{w2} - T_3) \quad (17)$$

where  $A_{e1}$ ,  $A_{e2}$ , and  $A_{e3}$  are the surface areas of each effect, and  $U_{e1}$ ,  $U_{e2}$ , and  $U_{e3}$  are overall heat transfer coefficients in each effect of the evaporator.

The above three equations calculate the surface area of each effect based on the transferred heat flux and the temperature difference in the heat exchanger of each effect. A total heat transfer coefficient is used, including all relevant thermal resistances between the condensing steam side and the evaporating solution side (heat transfer in the films of each side, as well as through the tube wall).

### 2.4. Equipment design and simulator outputs

The main parameters that the engineering team took into consideration are the temperatures inside the evaporation vessels. The design decision was finalized while also taking into account the economic criteria. It was mainly affected by the type of solar collectors that would provide the thermal energy to the first effect. Two basic types were considered: (a) parabolic trough collectors and (b) evacuated tube collectors. The cost of the former was very high, as the control system for such a small steam generation system was almost equivalent to the cost of the solar field itself. As a result, a special type of concentrated type of evacuated tube collectors was selected which could deliver hot water at 80°C.

This temperature could result in reasonable size of the heat exchanger inside the first vessel, in case a temperature of approximately 55°C was considered. As a result, through the use of the simulator tool, it was decided to design and operate the pilot brine treatment system at the following operating conditions:

- 1st effect: 55°C @ 0.15 bar (a);
- 2nd effect: 45°C @ 0.1 bar (a).

These operating conditions suggested that the following heat exchanger surface had to be used:

- 1st effect: 4 m<sup>2</sup>; and
- 2nd effect: 3 m<sup>2</sup>.

After having determined all major equipment parameters design values, the software model tool was used for the final design stage of the evaporator.

### 2.5. Detailed design of the evaporator vessels and heat exchangers

The evaporator consists of two effects, each operating in different pressure [5–15]. Each effect has cylindrical shape, placed vertically on the supporting scaffold. Inflowing brine is showered, equally distributed, upon the heating coils of the first effect. The heating element consists of U-shaped tubes, horizontally positioned in hexagonal arrangement. The heating element is connected to the evaporation effect via a flange, located eccentrically in one side of the cylinder.

A multi-layered structure above the heating element distributes equally the incoming brine flow across the length and width of the heater. The structure consists of three levels of perforated stainless

steel metal sheets, with diameters of 5.0, 3.0, and 2.0 mm from top to bottom, arranged in a grid across the surface of each level. The specific arrangement is designed to distribute the inflow with the minimum pressure drop.

The effects are arranged in vertical position. The chosen arrangement assists the flow of the waste concentrated brine (wcb) between effects, even at low pressure difference operation. Certain drawback of this arrangement is the overall height of the construction, if the design requires more effects.

Evaporation is taking place in series, inside the cylinders. The design considers 40% of the inflow to evaporate in the first effect. Inside the cylinder, steam is separated from the droplets and the remaining brine flows to the second effect. The remaining 33% of the brine is evaporated in the second effect. The decrease in the performance is due to the increase in the TDS content (elevation of the boiling point). The evaporation is performed in a single pass; there is no recirculation process.

Heat in the first effect is provided via hot water from the solar collectors. Hot water flows inside the heating coils with inflow temperature at 85°C. Inflow temperature can be regulated according to the solar heat available.

Designed temperature drop inside the coils is 10°C, while water flow can also be adjusted, according to each setup.

Heat in the second effect is provided via the steam from the first effect. Steam is condensed inside the coils of the second effect, under constant temperature. Due to the condensation, the overall heat transfer coefficient is improved, thus allowing smaller temperature differences. Condensed steam (distilled water) is further cooled in the sub-cooled region, with the use of two tube-in-tube heat exchangers, before it expands in the distilled water collection vessel. Without cooling, the production of steam due to expansion could be 7.0 m<sup>3</sup>/h. The specific heat exchangers have 1.0 kW capacity and also act as preheaters for the inflowing brine.

Steam from the second effect, after being separated from brine droplets, is condensed in a plate heat exchanger, with the use of cold brine from the RO unit. The condenser is also acting as a first stage preheater for the inflowing brine, as part of the brine is used as inflow in the system, while the rest is disposed to the sewage.

The remaining concentrated brine is collected in the concentrated brine vessel. The unit is equipped with two vessels for the collection of distilled water and brine in the final stage of the process. The same

vessels operate also as suction vessels for the vacuum pump. The final products are collected inside the vessels until the level reaches a certain height. Then, each liquid is removed via a centrifugal pump connected to the bottom of each vessel.

The dimensions of the collecting vessels are  $\Phi 400 \times 500$  mm, with effective height 400 mm.

The suction of the vacuum pump is attached on top of the two vessels. The technical specifications of the pump are based on the achievement of a logical start-up time (evacuation), and on the need of compensating the air leakages and non-condensable gases at steady state. Vacuum pump is selected according to the following data:

- Evacuation volume: 1,200 l
- Evacuation time: 6.0 min
- Air leakages: 0.5 kg/h (at steady state)
- Non-condensable gases: 0.025 g/kg of inflow.

## 2.6. Final evaporator design

The evaporator has a cylindrical shape with torispherical heads (Fig. 4). The length of the cylindrical section is 1,000 mm, while the overall length, with heads, is 1,200 mm. Effective volume of the evaporator is approximately 200 lt. The vessel is designed according to ASME standards for full vacuum, and tested with compressed air at 6 bar(a). The material used is EN 1.4410 (Super Duplex), with 5.0 mm thickness.

The heating element is mounted eccentrically in the head, via a flange with neck. The element consists of U-shaped tubes in a hexagonal arrangement. A custom-made stationary-head bonnet with pass partition separates the inflow and outflow. A small pitch of 1.25 is selected for the tube bundle arrangement, in order to achieve maximum density of the tube bundle, in the direction of the showered brine flow. The heating element is designed according to TEMA standards.

A diaphragm is attached to the upper middle of the cross-section, along the length of the cylindrical vessel, separating it in two sections. The tube bundle of the heating element is located in the left section, while the right section is free. As steam is created at the surface of the heating element, it is forced to move downwards, under the diaphragm, in order to exit the vessel. This movement, along with the small velocity in the right section assists the separation of the droplets from the steam. A cylindrically shaped plastic fibered demister separates further the droplets, sized above 0.1 m.

Evaporators are designed according to TEMA standards, as following:

- (1) System: TEMA BKU (Bonnet, Kettle type, U-tube bundle)
- (2) Class: TEMA C
- (3) Tubes:
  - (a) Pitch: 1.25 mm
  - (b) Pattern: triangular, 30°
  - (c) O.D.: 19.05 mm
  - (d) Thickness: 1.24 mm (according to TEMA RCB-2.31 and commercially available sizes)
  - (e) Material: EN 1.4410 (Duplex Stainless Steel)
  - (f) Length: 52.4 m per stage
  - (g) Total area: 7 m<sup>2</sup> (4 m<sup>2</sup> first effect, 3 m<sup>2</sup> second effect)
- (4) Vessel:
  - (h) Designed according to TEMA and ASME BPVC S.8
  - (i) Length: 1200.0 mm (total)
  - (j) O.D.: 478 mm
  - (k) Thickness: 5.0 mm (according to ASME BPVC for external pressure and commercially available sizes)
  - (l) Volume: 2001



Fig. 4. System during construction.

(5) Brine distribution system:

- (m) Custom design and according to CRANE TP-410 (experimentally confirmed)
- (n) 3 stages of brine distribution
- (o) Final stage composed of 133 holes  $\Phi$  2,0 mm, total area 0,41E-3 m<sup>2</sup>.

### 3. Automation—Operation control

Control of the system is performed via a PC-based SCADA interface. Multiple temperature and pressure transmitters are installed in key positions in the system, collecting all necessary data for the control of the operation. Data are collected in a PLC controller, with the necessary programming for the control of the unit. The PLC receives input from the following sensor equipment:

- Temperature transmitters inside the evaporators;
- Temperature transmitters in the hot water from solar field;
- Flow transmitters in the hot water from solar field;
- Flow transmitter in the inflowing brine (feed);
- Pressure transmitters inside the evaporators;
- Level transmitters inside the evaporators; and
- Level transmitters inside the concentrated brine and distillate vessels.

The PLC acts on the following equipment:

- Vacuum pump;
- Inflow pump;
- Inflow control valve; and
- Pressure control valve.

Evacuation pumps of the concentrated brine and distillate vessels.

A number of alarms are also installed regarding unwanted level increase inside the evaporators and vessels.

With the above-mentioned controls and the necessary PLC programming, the operation of the unit can be automated, eliminating the need for continuous supervision from a technician. During the operation of the unit, the vacuum pump starts at the beginning of the session, in order to evacuate the system, and then it is set into stand-by mode. The vacuum pump starts again when a pressure increase is detected, in order to remove non-condensable gases or any air intake due to leakages.

Inflow pump starts after the evacuation of the system. The inflow stream enters the condenser providing the necessary cooling for the process. Part of the

preheated brine enters the system for evaporation (feed), while the rest returns to the sewage. The necessary quantity of the inflowing brine (feed) for evaporation is automatically calculated by the system and controlled via a regulating valve. The inflow calculation is based on the energy balance of the system, taking into account the available heat from the solar field at any time, as follows:

$$E_{in} = E_{evap} \rightarrow m_{in} = \frac{m_{sc} \times C_p \times \Delta T}{2 \times h_{fg} \times (1 - p)}$$

where  $m_{in}$ : brine inflow [kg/h],  $m_{sc}$ : hot water flow from solar system,  $c_p$ : specific heat capacity [kJ/kgK],  $h_{fg}$ : specific latent heat@ $P_{evap}$  [kJ/kg],  $\Delta T$ : hot water temperature difference,  $p$ : waste brine ratio [%].

#### 4. Results

In Figs. 5 and 6, the results from the laboratory analyses carried out in the Unit of Environmental Science and Technology are given. More particularly, four different samples were collected and analyzed for the following physicochemical parameters: (a) pH (Fig. 5); (b) TDS; and (c) chlorides. The samples were collected after operation of the evaporator unit at the following dates: (a) 21.02.2013; (b) 26.04.2013; (c) 15.05.2013; and (d) 03.06.2013.

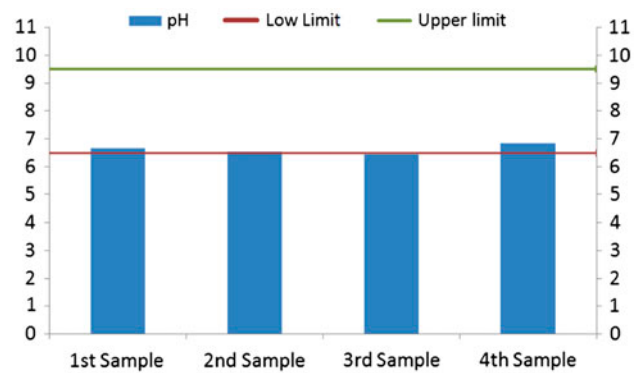


Fig. 5. pH measurement of the collected samples and limits of the Water Drinking Directive.

The instrumentation used for measuring both the conductivity and pH parameters was a Mettler Toledo MPC227. The measurements were based on the Standard Methods 4500-H and 2510.

##### 4.1. Results of pH measurements

The results and the upper and lower limits for drinking water (according to the Drinking Water Directive) are given in Fig. 5. As illustrated, a slight increase of pH will be required prior to potential water distribution for drinking purposes.

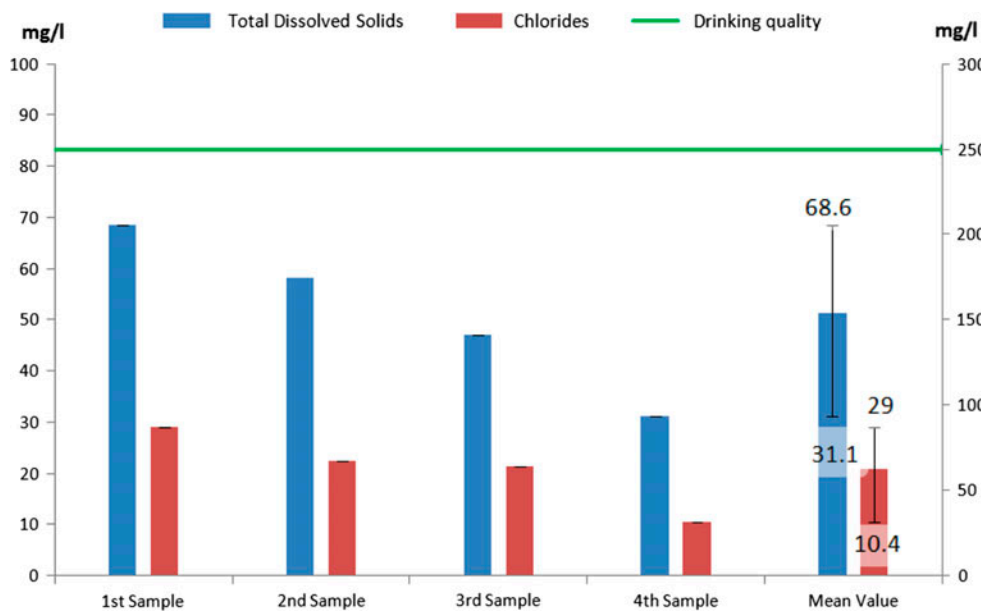


Fig. 6. TDS and chlorides of produced water from the evaporator (left axis) compared to drinking water quality (chlorides criterion, right axis) according to Drinking Water Directive.

#### 4.2. Results for chlorides and TDS

The results and the respective limit for drinking water quality (according to Drinking Water Directive) are given in Fig. 6. As illustrated, the quality of the produced water for these parameters is superior to the required standards.

#### Acknowledgments

This work has been carried out within the European project SOL-BRINE (LIFE09 ENV/GR/000299). Financial support by the European Commission under the European financial instrument for the environment, LIFE + is gratefully acknowledged.

#### Nomenclature

##### Latin symbols

$a$	— temperature-related drying kinetic constant
$A_{DHE}$	— exchanger surface area, $m^2$
$A_{ec}$	— surface area, $m^2$
$A_{e1}$	— surface area of 1st effect, $m^2$
$A_{e2}$	— surface area of 2nd effect, $m^2$
$A_{e3}$	— surface area of 3rd effect, $m^2$
$B^o$	— nucleation kinetic, 1/s
$bpr_1$	— boiling point elevation in 1st effect, $^{\circ}C$
$bpr_2$	— boiling point elevation in 2nd effect, $^{\circ}C$
$bpr_3$	— boiling point elevation in 3rd effect, $^{\circ}C$
$c$	— temperature-related drying kinetic constant
$C_{eq}$	— saturated concentration (per unit mass solution), $kg/kg$
$d$	— height of magma layer, $m$
$E_{co}$	— compressor electric power, $kW$
$F_a$	— drying air flow rate, $kg/s$
$f_v$	— volumetric shape factor
$G$	— crystal growth rate, $m/s$
$k$	— drying constant, $h^{-1}$
$k_G$	— crystal growth kinetic constant
$k_n$	— crystal nucleation kinetic constant
$k_o$	— drying kinetics constant
$L_d$	— dominant crystal length, $m$
$L_m$	— mean crystal length, $m$
$L_1$	— solution flow rate from 1st effect, $kg/s$
$L_2$	— Solution Flow Rate from 2nd effect, $kg/s$
$L_3$	— Solution Flow Rate from 3rd effect, $kg/s$
$m_{mix}$	— the output flow rate from the mixing of the three condensates of the evaporator, $kg/s$
$m_s$	— steam feed rate, $kg/s$
$m_{so}$	— steam flow rate, $kg/s$
$M_T$	— mass of crystals per unit volume of crystallizing solution, $kg/m^3$
$N$	— rotation speed, $Hz$
$n_o$	— nuclei population density, $m^{-3}$
$P_{cr}$	— crystallizer pressure, $atm$
$Q_c$	— heat flux for crystallizer, $kW$
$Q_{cd}$	— heat flux, $kW$
$Q_{ec}$	— heat flux, $kW$

$Q_{Fc}$	— volumetric feed rate in crystallizer, $m^3/s$
$Q_{e2}$	— heat flux in 2nd effect, $kW$
$Q_{e3}$	— heat flux in 3rd effect, $kW$
$R$	— vapor fraction feeding compressor, %
$R_c$	— ratio of molecular weight of hydrated salt per molecular weight of dehydrated salt
$t$	— drying time, $h$
$T_a$	— inlet air temperature in dryer, $^{\circ}C$
$T_{cr}$	— crystallizer temperature, $^{\circ}C$
$T_{condex}$	— exit temperature of the condensate from the preheater, $^{\circ}C$
$T_{mix}$	— exit water temperature after the mixing process, $^{\circ}C$
$T_1$	— solution temperature in the 1st effect, $^{\circ}C$
$T_2$	— Solution Temperature in 2nd effect, $^{\circ}C$
$T_3$	— solution temperature in 3rd effect, $^{\circ}C$
$T_m$	— magma temperature, $^{\circ}C$
$T_s$	— feed steam temperature, $^{\circ}C$
$u$	— air velocity in dryer, $m/s$
$U_{cd}$	— overall heat transfer coefficient, $kW/m^2^{\circ}C$
$U_{ec}$	— overall heat transfer coefficient constant, $kW/m^2^{\circ}C$
$U_{e1}$	— overall heat transfer coefficient in 1st effect, $kW/m^2^{\circ}C$
$U_{e2}$	— overall heat transfer coefficient in 2nd effect, $kW/m^2^{\circ}C$
$U_{e3}$	— overall heat transfer coefficient in 3rd effect, $kW/m^2^{\circ}C$
$V_{cr}$	— crystallizer volume, $m^3$
$V_{fr}$	— fraction of vaporized solvent per feed solution, $kg/kg$
$V_{scr}$	— vapor rate, $kg/s$
$V_1$	— vapor flow rate in 1st effect, $kg/s$
$V_2$	— vapor flow rate in 2nd effect, $kg/s$
$V_3$	— vapor flow rate in 3rd effect, $kg/s$
$W$	— solvent flow rate, $kg/s$
$W_D$	— moisture feed rate in the dryer, $kg/s$
$X$	— final moisture content of salt
$X_{cr}$	— concentration (inside crystallizer), $kg/kg$
$X_{cr}$	— concentration per unit mass solute, $kg/kg$
$X_{crf}$	— saturated concentration (per unit mass solvent), $kg/kg$
$X_M$	— magma moisture content, $kg/kg$
$X_1$	— solution concentration in 1st effect, $kg/kg$
$X_2$	— solution concentration in 2nd effect, $kg/kg$
$X_3$	— solution concentration in 3rd effect, $kg/kg$
$Y$	— crystal yield, $kg$

##### Greek letters

$\Delta Y$	— drying air absolute humidity increase, $kg/kg$ db
$\Delta H_m$	— heat of vaporization for moisture, $kJ/kg$
$\Delta T_{LM}^{DHE}$	— logarithmic mean temperature, $^{\circ}C$
$\Delta T_{LM}$	— logarithmic mean temperature, $^{\circ}C$
$\Delta H_s$	— heat of vaporization (condensation) of heating steam, $kJ/kg$
$\Delta H_1$	— heat of vaporization of solvent in 1st effect, $kJ/kg$

$\Delta H_2$	— heat of vaporization of solvent in 2nd effect, kJ/kg
$\Delta H_3$	— heat of vaporization of solvent in 3rd effect, kJ/kg
$\Delta H_{c1}$	— enthalpy of vaporization at crystallizer temperature, kJ/kg
$\Delta H_m$	— heat of vaporization for solvent, kJ/kg
$\Delta H_c$	— heat of crystallization, kJ/kg
$\Delta C$	— supersaturation, kg/kg
$\rho_1$	— density of inlet solution, kg/m <sup>3</sup>
$\rho_c$	— solid crystal density, kg/m <sup>3</sup>
$\rho_2$	— density of outlet solution, kg/m <sup>3</sup>
$\tau$	— residence time, s

## References

- [1] National Research Council, in: Desalination: A National Perspective, National Academy of Sciences, Washington, DC, 2008, pp. 90–120. Available from: <http://www.nap.edu/catalog/12184.html>.
- [2] Australian Government, National Water Commission, Emerging trends in desalination: A review, National Water Commission, October 2008. Available from: [http://www.nwc.gov.au/\\_\\_data/assets/pdf\\_file/0009/11007/Waterlines\\_-\\_Trends\\_in\\_Desalination\\_-\\_REPLACE\\_2.pdf](http://www.nwc.gov.au/__data/assets/pdf_file/0009/11007/Waterlines_-_Trends_in_Desalination_-_REPLACE_2.pdf).
- [3] A. Robertson, L. Duc Nghiem, Treatment of high TDS liquid waste: Is zero liquid discharge feasible? J. Water Sustain. 1 (2011) 153–163.
- [4] SOL-BRINE project, Deliverable 2.4: Technical report explaining the design procedure and the sizing of the brine treatment system. Available from: [uest.ntua.gr/solbrine/uploads/files/Deliverable2.4.pdf](http://uest.ntua.gr/solbrine/uploads/files/Deliverable2.4.pdf) (2012). Accessed October 10, 2013.
- [5] A. Gregorzewski, K. Genthner, E. Zarza, J. Leon, J. de Gunzbourg, G. Alefeld, J. Scharfe, The solar thermal desalination research project at the plataforma solar de Almeria, Desalination 82 (1991) 145–152.
- [6] T. Hodgkiss, Current status of materials selection for MSF distillation plants, Desalination 93 (1993) 445–460.
- [7] D. Annaratone, Pressure Vessel Design, Springer, Heidelberg, 2007.
- [8] Spirax Sarco, The Steam And Condensate Loop—An Engineer's Best Practice Guide For Saving Energy and Optimising Plant Performance, USA, 2011.
- [9] TEMA: Standards of the Tubular Exchanger Manufacturers Association, TEM, New York, NY, 2007.
- [10] R. Mukherjee, Effectively Design Shell-and-Tube Heat Exchangers. Available from: <http://www-unix.ecs.umass.edu/~rlaurenc/Courses/che333/Reference/exchanger.pdf> (1998). Accessed September 11, 2013.
- [11] VDI-GVC, VDI Heat Atlas, second ed., Springer-Verlag, Berlin, 2010.
- [12] B.M. Fabuss, A. Korosi, Boiling point elevations of sea water and its concentrates, J. Chem. Eng. Data 11 (1996) 606–609.
- [13] M.H. Sharqawy, J.H. Lienhard, S.M. Zubair, Thermophysical properties of seawater: A review of existing correlations and data, Desalin. Water Treat. 16 (2010) 354–380.
- [14] A. Cipollina, G. Micale, L. Rizzuti, (Eds.), Seawater Desalination. Green Energy and Technology, Springer-Verlag, Berlin, 2009.
- [15] W. Umrath, Fundamentals of Vacuum Technology. Available from: [http://isnap.nd.edu/Lectures/urls/LEYBOLD\\_FUNDAMENTALS.pdf](http://isnap.nd.edu/Lectures/urls/LEYBOLD_FUNDAMENTALS.pdf) (2007). Accessed October 11, 2013.